Coupling mass transfer with mineral reactions to investigate CO_2 sequestration in saline aquifers with non-equilibrium thermodynamics

Yuanhui Ji[1,*], Xiaoyan Ji[1], Xiaohua Lu[2], Yongming Tu[3,4]

[1] *Division of Energy Engineering, Luleå University of Technology, 971 87 Luleå, Sweden*
[2] *State Key Laboratory of Materials-Oriented Chemical Engineering, Nanjing University of Technology, 210009, Nanjing, P. R. China*
[3] *Key Laboratory of Concrete and Prestressed Concrete Structures of Ministry of Education, Southeast University, 210096, Nanjing, P. R. China*
[4] *Division of Structural Design and Bridges,Royal Institute of Technology (KTH),10044 Stockholm, Sweden*
** Corresponding author. Tel: +46 920491271, Fax: +46 920491074, E-mail: yuanhui.ji@ltu.se*

Abstract: The coupling behaviors of mass transfer of aqueous CO_2 with mineral reactions of aqueous CO_2 with rock anorthite are investigated by chemical potential gradient and concentration gradient models, respectively. SAFT1-RPM is used to calculate the fugacity of CO_2 in brine. The effective diffusion coefficients of CO_2 are obtained based on the experimental kinetic data reported in literature. The calculation results by the two models and for two cases (mass transfer only and coupling mass transfer with mineral reaction) are compared. The results show that there are considerable discrepancies for the concentration distribution with distance by the concentration gradient and chemical potential gradient models, which implies the importance of consideration of the non-ideality. And the concentrations of aqueous CO_2 at different distances by the concentration gradient model are higher and further than that by the chemical potential gradient model. The mineral reaction plays a considerable role for the CO_2 geological sequestration when the time scale reaches 10 years for the anorthite case.

Keywords: *CO_2 geological sequestration, Non-equilibrium thermodynamics, Chemical potential gradient, Mass transfer, Geochemical reaction*

1. Introduction

Geological sequestration of anthropogenic CO_2 is a promising carbon mitigation strategy[1, 2], which includes the injection of CO_2 into deep saline aquifers, depleted oil and gas reservoirs, and deep coal seams[2, 3], and the storage in deep saline aquifers seems to have the largest potential capacity[3, 4, 5]. The four main CO_2 sequestration mechanisms in deep saline aquifers proposed are solubility trapping; capillary trapping; hydrodynamic trapping and mineral trapping[1, 2]. In order to study the long-term behaviors of CO_2 in formations, and to estimate the possible CO_2 leakage risk, it is necessary to investigate the dissolution of CO_2 in brine, the mass transfer of dissolved CO_2 and the coupling behaviors of mass transfer with the mineral reactions of aqueous CO_2 with rocks over a wide range of spatial and temporal scales[1, 3, 6-8].

Phase equilibria of CO_2 in water and brines have been widely studied[9-12]. The molecular-based statistical associating fluid theory (SAFT) equation of state (EOS) is a promising model for systems up to high pressures, which represents the density and phase equilibrium for CO_2-H_2O from 285 to 473 K and up to 600 bar, and for CO_2-H_2O-NaCl from 298 to 373 K and up to 200 bar[10, 13]. For the kinetics research, numerous investigations on the mass transfer of CO_2 in high-pressure water or brines have been conducted to simulate CO_2 geological or ocean disposal processes[5, 14-16]. Yang and Gu[5] studied CO_2 dissolution in brine at elevated pressures experimentally and described the mass transfer of CO_2 in brine using Fick's Second Law with an effective diffusion coefficient considering the effect of convection, which are two orders of magnitude larger than the molecular diffusivity of CO_2 in water[5], and it implies that the density-driven natural convection greatly accelerates the mass transfer of CO_2 in brines. Generally, mass transfer flux is described with concentration gradient as the driving

force. However, in real systems, Fick's law must be amended to account for nonideal behavior. So the driving force for solute fluxes is not the concentration gradient, but the chemical potential gradient[17, 18]. Our previous work[19, 20] also reveals that it is necessary to consider the non-ideality of the complicated systems. Therefore, on the basis of the work by Yang and Gu[5], the mass transfer of CO_2 in brines is investigated by chemical potential gradient model[21] based on derivation of $\partial a_i/\partial t$ (a_i is the activity of species i). The calculated results show the importance of the consideration of the non-ideality. Moreover, path-of-reaction and kinetic modeling of CO_2-brine-mineral reactions in deep saline aquifers have been conducted[9, 22-25]. The nonisothermal reactive transport code TOUGHREACT[26, 27] were developed which introduced reactive chemistry into the multi-phase fluid and heat flow code TOUGH2[28].

In this paper, the coupling behaviors of the mass transfer of aqueous CO_2 with the typical mineral reactions of aqueous CO_2 with rocks will be investigated and analyzed by chemical potential gradient and concentration gradient models, respectively.

2. Thermodynamic model

The fugacities of the aqueous CO_2 are calculated using SAFT1-RPM EOS[13] and the details are described in literature[13].

3. Kinetics modeling

3.1. Model description

3.1.1. Mass transfer

Concentration gradient model

The flux generalized to three dimensions is described as[18, 29]

$$J_i = -D_C \nabla C_i \tag{1}$$

where, J_i is molar flux of species i; D_C is the effective diffusion coefficients in concentration gradient model; C_i is the molar concentration of species i.

Chemical potential gradient model

As described in above text, in real systems, chemical potential gradient is the driving force for solute fluxes[17, 18], and the flux generalized to three dimensions is described as[18, 29]

$$J_i = -(D_\mu C_i / RT) \nabla \mu_i \tag{2}$$

where, J_i is molar flux of species i; D_μ is the effective diffusion coefficients in chemical potential gradient model; μ_i is the chemical potential of species i and described by Eq. (3)[30].

$$\mu_i = \mu_i^0 + RT\ln(f_i / f_i^0) = \mu_i^0 + RT\ln a_i \tag{3}$$

where, μ_i^0, a_i, f_i and f_i^0 are the standard chemical potential, activity, fugacity and standard fugacity of component i, respectively. At a certain T and P, both μ_i^0 and f_i^0 are constants. In this paper, one-dimensional case is studied, and the convective molar flux by the bulk motion of the fluid is not added in Eqs. (1) and (2), but an effective diffusion coefficient considering the effect of convection is used. Combining Eq. (2) with Eq. (3), Eq. (4) can be obtained.

$$\boldsymbol{J_i = -\frac{D_\mu C_i}{RT}\nabla(RT \ln f_i) = -D_\mu C_i \nabla \ln f_i} \tag{4}$$

Diffusion coefficient determination

The effective diffusion coefficient is obtained based on the experimental kinetic data in Test 4 reported by Yang and Gu[5]. At the temperature and different pressures of Test 4, the quantitative relations of fugacities of aqueous CO_2 with their concentrations are determined from fitting according to the calculation results by SAFT1-RPM EOS[13] with a function form as $f_{CO2(aq)}=a+b\cdot C_{CO2(aq)}$ in which a and b are parameters at a certain temperature and pressure. The aqueous CO_2 concentrations at the interface are calculated with SAFT1-RPM[13] by assuming instantaneous saturation of CO_2[21]. In the work of Ref. [5], the CO_2 dissolution was performed in a PvT cell with a cross-sectional area A (7.9273×10^{-4} m^2) and brine phase height H (0.0442 m), the CO_2 pressures P_t at different time t were recorded. The number of moles of dissolved CO_2 (n_t) are determined from the gaseous pressure at different time t and the initial experimental conditions. Based on the mass balance, Eq. (5) can be obtained.

$$\int_0^x C_{CO_2(aq)} A dx = n_t \tag{5}$$

where $C_{CO2(aq)}$ ($mol\cdot m^{-3}$) is the concentration of aqueous CO_2 in brines, and A (m^2) is the contact area of gaseous CO_2 with brine and is assumed to be the cross-sectional area of the cell, and x (m) is the mass transfer distance. In the work of Yang and Gu[5], only the experimental kinetics data after 180s were used to analyze the mass-transfer process of CO_2 in the brine. In this paper, we also take the flux J and n_t after 180s.

According to the flux J and n_t at different pressures in Test 4[5] and combining Eqs. (1) with (5), the effective diffusion coefficient at respective pressures in the one-dimensional concentration gradient model can be determined directly. While for the effective diffusion coefficient in the chemical potential gradient model, a simple but effective method, direct search method, can be used, in which the initial value and step length of the effective diffusion coefficient are assumed as 1.0×10^{-9} $m^2\cdot s^{-1}$, while the maximum value is 1.0×10^{-6} $m^2\cdot s^{-1}$. The minimum, maximum values and step length of the distance x are assumed as 1.00×10^{-6}, H and 5.00×10^{-4} m. Then according to the flux J and n_t at different pressures in Test 4[5] and combining Eqs. (4) and (5), the effective diffusion coefficient at respective pressures can be determined by the numerical simulation calculation.

3.1.2. Mineral reaction rate

Mineral reaction

Mineral trapping is the fixing of CO_2 in carbonate minerals due to a series of geochemical reactions[9, 31]. It is reported that the most promising reactions for mineral trapping involve the minerals which provide divalent cations (Ca^{2+}, Mg^{2+}, Fe^{2+}) for precipitation of carbonate[9, 31]. One of the most common sedimentary-mineral sources of divalent cations is anorthite and is studied as a case in this paper. The mineral trapping takes place due to the following reactions as demonstrated by the example of anorthite dissolution:

Dissolution of CO_2 acidifies formation water through the following reaction[31].

$$CO_2(aq)+H_2O \rightleftharpoons H_2CO_3 \rightleftharpoons HCO_3^- + H^+ \rightleftharpoons CO_3^{2-} + 2H^+ \tag{6}$$

Aqueous CO_2 dissociates in water and produces carbonic acid, bicarbonate and carbonate ions, the acid attacks anorthite, leaching Ca^{2+} and neutralizing the acid through Reaction (7)[9, 31].

$$CaAl_2Si_2O_8 + 2H^+ + H_2O \rightleftharpoons Ca^{2+} + Al_2Si_2O_5(OH)_4 \tag{7}$$

The divalent cations precipitates as calcium carbonate through Reactions (8) and (9)[9, 31].

$$Ca^{2+} + HCO_3^- \rightarrow CaCO_3 + H^+ \quad (8)$$

$$Ca^{2+} + CO_3^{2-} \rightarrow CaCO_3 \quad (9)$$

In this work, Eq. (7) and the following net reaction are considered to study the mineral reaction rate.

$$Ca^{2+} + CO_2(aq) + H_2O \rightarrow CaCO_3 + 2H^+ \quad (10)$$

Mineral reaction rate

According to nonequilibrium thermodynamics, the chemical reaction rate of a single reaction is described as Eq. (11)[32],

$$\text{Rate} = R_f (1 - e^{-A/RT}) \quad (11)$$

where, R_f is the forward rate of the reaction, A is the affinity and is described as the negative of the molar Gibbs free energy change of reaction, R is the gas constant, T is the temperature. Based on Eq. (11), the general rate equation for geochemical reaction kinetics is[22, 24]:

$$\mathbf{Rate} = (1/V) \cdot \mathrm{d}n_i / \mathrm{d}t = (1/V) \cdot K \cdot A_{\min} \cdot \exp(-E_a / RT) \cdot [1 - \frac{Q}{K_{eq}}] \quad (12)$$

where, V is the volume of brines, K is the rate constant, $A_{\min}$ is the reactive surface area, E_a is the activation energy, Q is the activity product and is described through Eq. (13), and K_{eq} is the equilibrium constant.

$$Q = \frac{[H^+]}{[Ca^{2+}] \cdot f_{CO_2(aq)}} \quad (13)$$

In Eq. (13), $[H^+]$ and $[Ca^{2+}]$ are the molar concentrations of H^+ and Ca^{2+} ions, respectively.

Mineral reaction rate parameters

Anorthite is chosen for a case study. The volume of brines is assumed as 1 m^3 (approximately equals to 1 kg). The rate constant, activation energy and specific reactive surface area of the rocks used are taken from literature[23] and shown in Table 1. The water:rock ratio is fixed at 1 kg water per 15 kg of rock[24]. The gas constant is taken as 8.3145 $J \cdot mol^{-1} \cdot K^{-1}$. The effect of temperature on the mineral reaction rate is neglected and the temperature is taken as 298.15K. In the calculation of Q, $[H^+]$ and $[Ca^{2+}]$ are taken from the pH value and composition of Rose Run brines[22]. The fugacities of aqueous CO_2 are determined by SAFT1-RPM EOS[13]. According to the equilibrium constants of the following Eqs. (14) and (15), the equilibrium constant of Eq. (10) can be obtained as shown in Eq. (16).

$$CO_2(aq) + H_2O \rightarrow HCO_3^- + H^+ \quad \log K(298.15K) = -6.37 \quad (14)$$

$$CaCO_3(calcite) + H^+ \rightarrow Ca^{2+} + HCO_3^- \quad \log K(298.15K) = 1.71 \quad (15)$$

$$Ca^{2+} + CO_2(aq) + H_2O \rightarrow CaCO_3 + 2H^+ \quad \log K(298.15K) = -8.08 \quad (16)$$

Table 1. The mineral considered and its reaction rate constant (K), activation energy (Ea) and specific reactive surface area[23].

Mineral	K ($mol \cdot m^{-2} \cdot s^{-1}$)	Ea ($J \cdot mol^{-1}$)	Specific reactive surface area ($m^2 \cdot g^{-1}$)
Anorthite	7.6×10^{-10}	1.78×10^{4}	1.00×10^{-3}

3.1.3. Model of coupling mass transfer with mineral reaction

The model of coupling mass transfer with mineral reaction can be derived from the equation of continuity for species *i* in a multicomponent reacting mixture as shown in Eq. (17)[29].

$$\frac{\partial C_i}{\partial t} = -(\nabla \cdot J_i) - r_i \tag{17}$$

where, r_i is the consumption rate of *i* by reaction. According to the different flux forms of Eqs. (1) and (4) and the reaction rate form of Eq. (12), the concentration gradient and chemical potential gradient models of coupling mass transfer with mineral reaction can be obtained.

3.2. Initial and boundary conditions

The initial condition is given by Eq. (18)

$$C_i(x,t)\big|_{t=0} = \begin{cases} C_{i0} & (x=0) \\ 0 & (x>0) \end{cases} \tag{18}$$

where, C_{i0} is the aqueous CO_2 saturated concentration. The left boundary conditions are the interface concentrations of aqueous CO_2 calculated with SAFT1-RPM[13] by assuming instantaneous saturation of CO_2[21]. The right boundary condition is

$$\frac{\partial C_i(x,t)}{\partial x}\Big|_{x=x_R} = 0 \quad (t>0) \tag{19}$$

where, x_R represents the distance between the right boundary and the interface.

3.3. Numerical solution

The partial differential equations are solved numerically using the built-in "pdepe" in the MATLAB program, which solves initial-boundary value problems for systems of parabolic and elliptic partial differential equations. The diffusion coefficient is taken the value calculated in this paper at 7.5322 MPa and the other experimental conditions of Test 4[5].

4. Results and Discussions

4.1. Effective diffusion coefficient

The effective diffusion coefficients at different pressures and other experimental conditions of Test 4[5] are calculated and shown in Fig. 1. Fig. 1 shows that the effective diffusion coefficients by both concentration gradient and chemical potential gradient models are close to each other and decrease with increasing pressure. Moreover, the effective diffusion coefficients calculated in this paper are close to that in our previous work by the chemical potential gradient model based on the derivation of $\partial a_i/\partial t$[21].

4.2. Concentration distribution by concentration and chemical potential gradient models

The concentration distribution of aqueous CO_2 with distance at 10 and 20 years through the concentration gradient and chemical potential gradient models coupling mass transfer with mineral reaction is shown in Fig. 2. From Fig. 2, there are considerable discrepancies for the concentration distribution with distance by the two models, which implies the importance of the consideration of non-ideality. The concentrations of aqueous CO_2 by the concentration gradient model are higher and further than that by the chemical potential gradient.

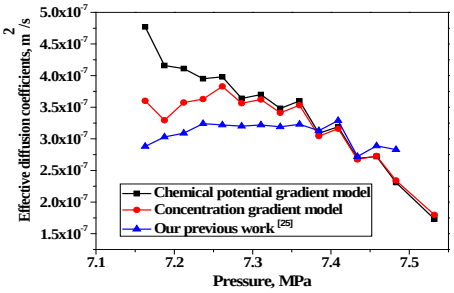

Fig. 1. Calculated effective diffusion coefficients at different pressures

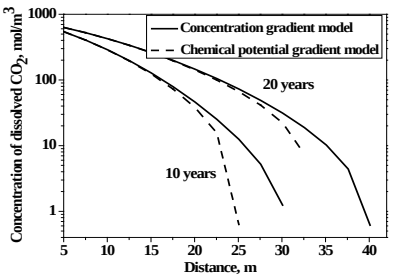

Fig. 2. Concentration distribution with distance for coupling mass transfer with mineral reaction.

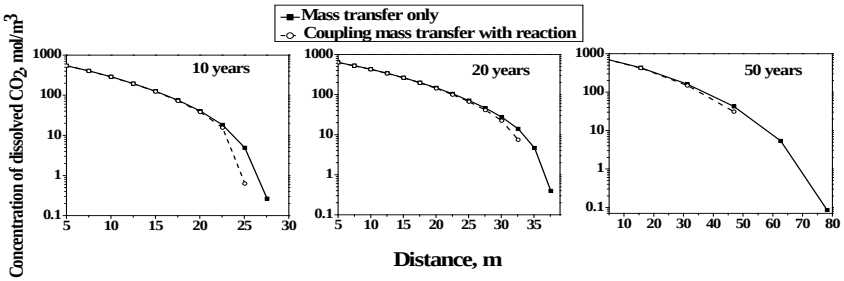

Fig. 3. C alculated concentration distribution with distance at different time scales in which two different cases are considered (1) mass transfer only; (2) coupling mass transfer with mineral reaction.

4.3. Concentration distribution by chemical potential gradient model for two cases: mass transfer only and coupling mass transfer with mineral reaction.

The concentration distribution of aqueous CO_2 with distance at 10, 20, 50 years by the chemical potential gradient model for two cases (mass transfer only and coupling mass transfer with mineral reaction) is shown in Fig. 3. From Fig. 3, for the anorthite case, it is observed that the mineral reaction plays a considerable role for the geological sequestration when the time scale reaches 10 years. Moreover, our results show that the mineral reaction does not bring obvious effect on the concentration distribution of aqueous CO_2 for time scale less than 10 years, and when the time scale is 1000 years, the aqueous CO_2 by the mass transfer can be completely reacted by the model rock anorthite due to the neglection of the effects of hydrodynamics and gravity. In future work, more types of rocks and the effects of hydrodynamics and gravity should be considered.

5. Conclusions

In this paper, the coupling behaviors of the mass transfer of aqueous CO_2 with the mineral reactions of aqueous CO_2 with model rock anorthite are investigated by chemical potential gradient and concentration gradient models, respectively. The effective diffusion coefficients of CO_2 are obtained based on the experimental kinetic data reported in literature. The results

show that there are considerable discrepancies for the concentration distribution with distance by the concentration gradient and chemical potential gradient models, which implies the importance of the consideration of the non-ideality. And the concentrations of aqueous CO_2 at different distances by the concentration gradient model are higher and further than that by the chemical potential gradient. The mineral reaction plays a considerable role for the geological sequestration when the time scale reaches 10 years for the anorthite case.

Acknowledgment

The authors thank Luleå University of Technology, the Swedish Research Council, the National Basic Research Program of China (2009CB226103), the National Natural Science Foundation of China (50808039) and the Natural Science Foundation of Jiangsu Province, China (BK2009138) for the financial supports.

References

[1] D. P. Schrag, Preparing to capture carbon, Science 315, 2007, pp. 812-813.

[2] A. Firoozabadi, P. Cheng, Prospects for subsurface CO_2 sequestration, AIChE J. 56, 2010, pp. 1398-1405.

[3] R. G. Jr. Bruant, A. J. Guswa, et al. Safe storage of CO_2 in deep saline aquifers, Environ. Sci. Technol. 36(11), 2002, pp. 240A-245A.

[4] S. Bachu, J. J. Adams, Sequestration of CO_2 in geological media in response to climate change: capacity of deep saline aquifers to sequester CO_2 in solution, Energy Convers. Manage. 44, 2003, pp. 3151-3175.

[5] C. Yang, Y. Gu, Accelerated mass transfer of CO_2 in reservoir brine due to density-driven natural convection at high pressures and elevated temperatures, Ind. Eng. Chem. Res. 45, 2006, pp. 2430-2436.

[6] S. M. V. Gilfillan, B. S. Lollar, et al. Solubility trapping in formation water as dominant CO_2 sink in natural gas fields, Nature 458, 2009, pp. 614 -618.

[7] D. W. Keith, J. A. Giardina, et al. Regulating the underground injection of CO_2, Environ. Sci. Technol. 39, 2005, pp. 499A-505A.

[8] C. M. Oldenburg, Transport in geologic CO_2 storage systems, Transp. Porous Med. 82, 2010, pp. 1-2.

[9] B. Zerai, CO_2 sequestration in saline aquifer: geochemical modeling, reactive transport simulation and single-phase flow experiment. Doctoral Dissertation, January, 2006.

[10] Y. H. Ji, X. Y. Ji, et al. Progress in the study on the phase equilibria of the CO_2-H_2O and CO_2-H_2O-NaCl systems. Chin. J. Chem. Eng., 15(3), 2007, pp. 439-448.

[11] N. A. Darwish, N. Hilal, A simple model for the prediction of CO_2 solubility in H_2O-NaCl system at geological sequestration conditions, Desalination 260, 2010, pp. 114-118.

[12] N. N. Akinfiev, L. W. Diamond, Thermodynamic model of aqueous CO_2-H_2O-NaCl solutions from 22 to 100 degrees C and from 0.1 to 100 MPa, Fluid Phase Equilibria 295, 2010, pp. 104-124.

[13] X. Y. Ji, S. P. Tan, et al. SAFT1-RPM approximation extended to phase equilibria and densities of CO_2-H_2O and CO_2-H_2O-NaCl systems. Ind. Eng. Chem. Res. 44, 2005, pp. 8419-8427.

[14] B. Arendt, D. Dittmar, R. Eggers, Interaction of interfacial convection and mass transfer effects in the system CO_2-water, Int. J. Heat Mass Transfer 47, 2004, pp. 3649-3657.

[15] R. Farajzadeh, H. Salimi, et al. Numerical simulation of density-driven natural convection in porous media with application for CO_2 injection projects, Int. J. Heat Mass Transfer 50, 2007, pp. 5054-5064.

[16] R. Farajzadeh, P. L. J. Zitha, J. Bruining, Enhanced mass transfer of CO_2 into water: experiment and modeling, Ind. Eng. Chem. Res. 48, 2009, pp. 6423-6431.

[17] N. Kocherginsky, Y. K. Zhang, Role of standard chemical potential in transport through anisotropic media and asymmetrical membranes, J. Phys. Chem. B 107, 2003, pp. 7830-7837.

[18] G. A. Truskey, F. Yuan, D. F. Katz., Transport phenomena in biological systems. Prentice Hall, 2009.

[19] C. Liu, Y. Ji, et al. Thermodynamic analysis for synthesis of advanced materials. Molecular Thermodynamics of Complex Systems, Struct Bond 131, 2009, pp. 193-270.

[20] Y. H. Ji, X. Y. Ji, et al. Modelling of mass transfer coupling with crystallization kinetics in microscale, Chem. Eng. Sci. 65(9), 2010, pp. 2649-2655.

[21] Y. H. Ji, X. Y. Ji, X. H. Lu, Modeling mass transfer of CO_2 in brine at high pressures by chemical potential gradient, Fluid Phase Equilibria 2010 submitted.

[22] B. Zerai, B. Z. Saylor, G. Matisoff, Computer simulation of CO_2 trapped through mineral precipitation in the Rose Run Sandstone, Ohio, Applied Geochemistry 21, 2006, pp. 223-240.

[23] F. Gherardi, T. Xu, K. Pruess, Numerical modeling of self-limiting and self-enhancing caprock alteration induced by CO_2 storage in a depleted gas reservoir, Chemical Geology 244, 2007, pp. 103-129.

[24] R. T. Wilkin, D. C. Digiulio, Geochemical impacts to groundwater from geologic carbon sequestration: controls on pH and inorganic carbon concentrations from reaction path and kinetic modeling, Environ. Sci. Technol. 44, 2010, pp. 4821-4827.

[25] T. Xu, Y. K. Kharaka, et al. Reactive transport modeling to study changes in water chemistry induced by CO_2 injection at the Frio-I Brine Pilot, Chemical Geology 271, 2010, pp. 153-164.

[26] T. Xu, K. Pruess, Modeling multiphase non-isothermal fluid flow and reactive geochemical transport in variably saturated fractured rocks: 1. Methodology. Am. J. Sci. 301, 2001, pp. 16-33.

[27] T. Xu, E. L. Sonnenthal, et al. TOURGHREACT: a simulation program for non-isothermal multiphase reactive geochemical transport in variably saturated geologic media. Comp. Geosci. 32, 2006, pp. 145-165.

[28] T. Xu, J. A. Apps, K. Pruess, Numerical simulation to study mineral trapping for CO2 disposal in deep aquifers. Appl. Geochem. 19, 2004, pp. 917 – 936.

[29] R. B. Bird, W. E. Stewart, et al. Transport Phenomena, John Wiley & Sons, Inc., 2006.

[30] J.M. Prausnitz, R.N. Lichtenthaler, E.G. de Azevedo, Molecular Thermodynamics of Fluid-phase Equilibria. Third edition, NJ, Prentice Hall PTR, 1999.

[31] J. M. Matter, P. B. Kelemen, Permanent storage of carbon dioxide in geological reservoirs by mineral carbonation, Nature Geoscience 2, 2009, pp. 837 – 841.

[32] D. Kondepudi, I. Prigogine, Modern Thermodynamics: From Heat Engines to Dissipative Structures. John Wiley & Sons, Chichester, 1998.